Journal of Physics: Conference Series **126** (2008) 012089 doi:10.1088/1742-6596/126/1/012089

Can direct electron detectors outperform phosphor-CCD systems for TEM?

Grigore Moldovan, Xiaobing Li and Angus Kirkland

Department of Materials, University of Oxford, Parks Road, Oxford, OX1 3PH, UK

E-mail: grigore.moldovan@materials.ox.ac.uk

Abstract. A new generation of imaging detectors is being considered for application in TEM, but which device architectures can provide the best images? Monte Carlo simulations of the electron-sensor interaction are used here to calculate the expected modulation transfer of monolithic active pixel sensors (MAPS), hybrid active pixel sensors (HAPS) and double sided Silicon strip detectors (DSSD), showing that ideal and nearly ideal transfer can be obtained using DSSD and MAPS sensors. These results highly recommend the replacement of current phosphor screen and charge coupled device imaging systems with such new directly exposed position sensitive electron detectors.

1. Introduction

Major achievements have been made over the last ten years in correcting the lens aberrations in transmission electron microscopy (TEM), thus increasing the performance of the instrument up to a level where the imaging detector become the major limiting factor. Because of their intrinsic design, current phosphor coupled charge-coupled-devices (CCD) detection systems suffer from a number of limitations, including poor resolution and efficiency, slow frame-rate and reduced field of view [1]. A new generation of sensors is now emerging from directly exposed sensors, based on a number of devices designed for position sensitive particle detection [2-4]. However a rather complex choice is being presented, as these detectors are rather fragmented in a number of architectures.

This work addresses two major questions in this field, can any of these new sensors provide sufficient improvements to justify replacement of the current detectors and, if so, which of these detection architectures is most suited for TEM? A brief introduction will be provided for the three major candidates, followed by detailed Monte Carlo-based calculations of their performance, which is discussed in terms of modulation transfer function for 200 keV electrons.

2. Direct Electron Detectors

Three major types of direct detectors are now being investigated for imaging in TEM, monolithic active pixel sensors (MAPS) [2], hybrid active pixel sensors (HAPS) [3] and double-sided strip detectors (DSSD) [4]. MAPS devices (Figure 1a) incorporate in each pixel most of the functions required for particle detection, i.e. charge generation and collection, pre-amplification, pulse shaping, analog-to-digital conversion, noise discrimination and signal integration. In comparison with CCDs, this not only provides faster frame rate, but also an added flexibility, such as the capacity of reading out only a specified region of interest. As a deviation from standard MAPS fabrication, a radiation-hard design and process is needed for their application in TEM.

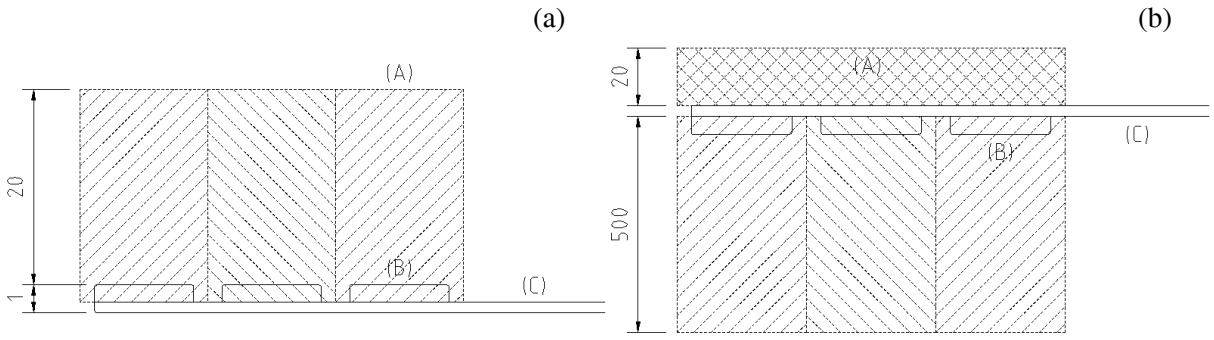

Figure 1: cross-sectional diagrams of (a) monolithic and (b) hybrid active pixel sensors, showing electron sensitive layer (A), pixel electronics (B) and interconnect and read-out (C). The sensitive layer of the hybrid sensor is separate and bonded on the read-out chip. Dimensions are in μm.

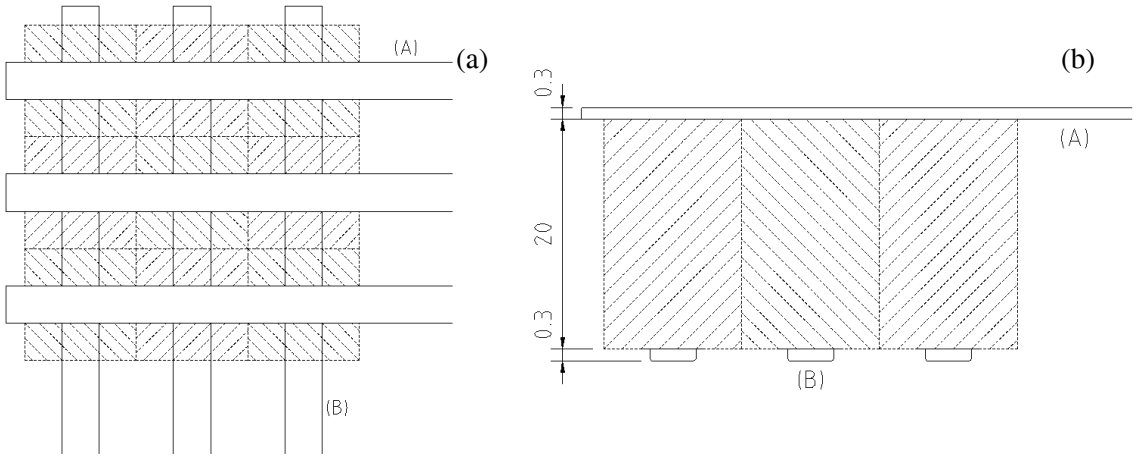

Figure 2: (a) plan-view and (b) cross-sectional diagrams of double sided Silicon strip detector. Orthogonal top (A) and bottom (B) strips are used to collect the induced charge from the sensitive volume (C), without the need of any read-out electronics in the beam path. Dimensions are in μm.

Because of the high costs associated with the development and manufacture of radiation-hard MAPS, a more flexible approach was introduced with HAPS (Figure 1b), where the radiation sensitive layer is separated from the active pixel read-out. This allows the use of a wide range of geometries and materials for sensing purposes and thus the application to a much wider range of radiation types and energies. Due to their low manufacture yield, current MAPS and HAPS detectors suffer from poor scalability, but it is hoped that developments in device fabrication will eventually overcome this problem.

The more traditional DSSD (Figure 2) offer a simple route around the problems of radiation-hard electronics and scalability, as the read-out system does not sit in the beam path and the device processing is simple and reliable. In contrast with CCD, MAPS and HAPS, DSSD is a counting detector where the position of each incoming particle is determined from the charge accumulated on orthogonal top and bottom collection strips. Because of this, DSSD is capable of on-board on-the-fly event discrimination, such as rejection of double counting.

3. Monte Carlo Simulations and Discussion

The electron scattering model used in these simulations follows Joy's model, which considers straight electron trajectories between discrete elastic Rutherford scattering events. Inelastic scattering is modeled by assuming a continuous energy loss along these trajectories. Accurate relativistic corrections to the Rutherford and Bethe formula are used, as well as the generation of fast secondary electrons. The usually small directional changes in inelastic scattering events are neglected [1]. For an adequate comparison, all the devices simulated here have a sensitive layer with a thickness of 20 μm and a collection pitch of 20 μm. The additional layers in each device structure are taken into account, as detailed in Figs. 1-2. Initial electron energy of 200 keV is considered here.

Figure 3 shows simulated trajectories of 10 electrons impinging on the sensitive layers of these detectors. MAPS and DSSD devices show the same type and distribution of trajectories (Figure 3a), due to their almost identical structure. Some of the primary electrons have a relatively straight trajectory, but most electrons suffer scattering events that displace them laterally up to 10 μm. Secondary electrons can be produced along this trajectory, and such an event can be observed in this set. Back-scattered yield is low. A somewhat similar distribution of trajectories is observed for the case of HAPS (Figure 3b), with the added scattering induced by the thick read-out chip that supports the sensitive layer. This additional scatting is sufficiently strong to occasionally deviate the primary electrons back into the sensitive layer and increase the back-scattered yield. Two such examples are present in this set of 10 electrons. The corresponding trajectories have a much larger lateral displacement, up to 100 μm for this case.

The generation of charge pairs along the electron trajectory was recorded in the detector plane, and average charge distributions in the central and neighboring pixel columns for each detector type are presented in Figure 4a. This data was obtained averaging over 100,000 simulated primary electrons, with an impact position randomly distributed across the central pixel. Because the sensors considered here are very thin, charge diffusion during charge collection is very limited and the distribution of induced charge carriers is the point spread function of the detector. The MAPS and DSSD sensors show the essentially same narrow charge distribution, again due to their very similar structure. Their point spread function is very sharp, with three pixels above the level of 100 electron-hole pairs/column. The HAPS detector shows a much wider charge distribution associated with the additional scattering in the thick support, with 11 pixels above the same signal level.

One of the most important metrics in detector performance is transfer of modulation from the object to the image as a function of spatial frequency, where the higher the modulation transfer, the better. Since MAPS and HAPS are integrating devices, their modulation transfer function is determined directly by their lateral charge distribution (Figure 4b). Whist MAPS shows a very good modulation transfer that decreases almost linearly to 0.33 at Nyquist limit, HAPS displays a rather

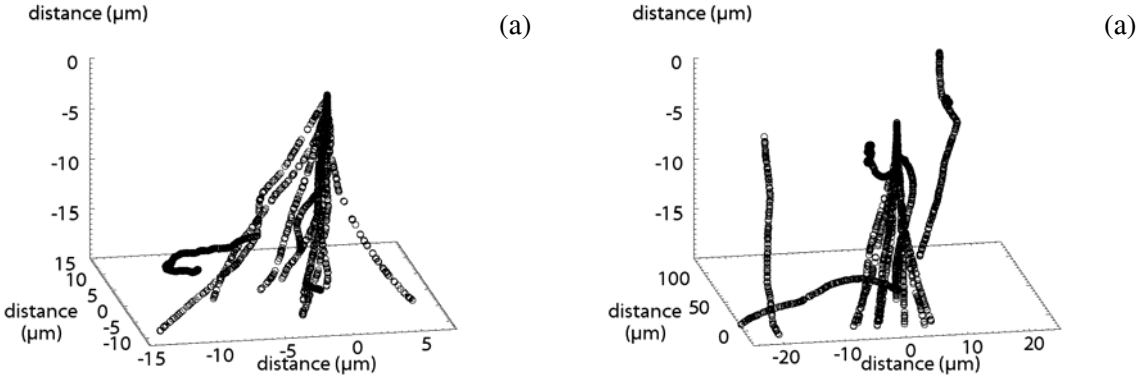

Figure 3: three-dimensional plots of simulated trajectories of 10 electrons with an entry energy of 200keV in the sensitive volume of (a) MAPS and SSD, and (b) HAPS, as presented in Figs. 1a-b, 2b.

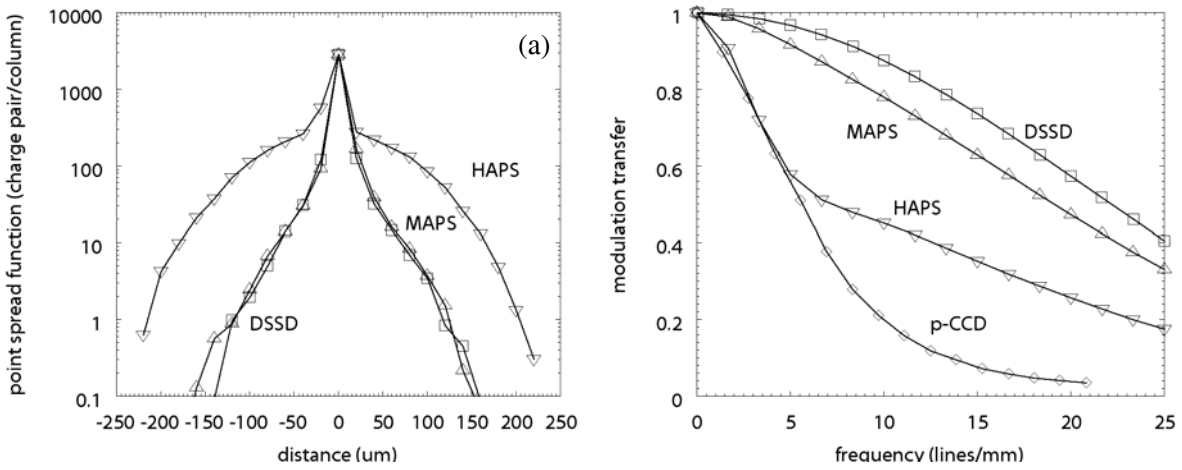

Figure 4: calculated (a) point spread function and (b) modulation transfer function of MAPS, HAPS and SSD detectors presented in Figs 1-2, in comparison with those of a typical phosphor-CCD system. Frequency in lines/mm corresponds to a pixel size of 20 μm.

poor transfer, which decreases rapidly to about 0.6 at 5 lines / mm and then slower to 0.18 at Nyquist. Since DSSD is a counting detector, it can use event discrimination to reject events in which two or more pixels are triggered for the same primary electron and retain an ideal modulation transfer that decreases only to 0.41 at Nyquist. These values compare with a rapidly decreasing modulation transfer, down to only 0.04 at Nyquist for a 24 μm pitch phosphor-CCD systems [1]. Note that the improvement in DSSD performance over that of MAPS is obtained at the expense of efficiency, but since efficiency is strongly influenced by the electronic noise particular to each device type, design and processing, a discussion on efficiency is not pursued here.

4. Conclusion

Calculations based on Monte Carlo simulations of electron-sensor interaction have been used to show that the modulation transfer of all direct detectors considered here for application in TEM is superior to that of current phosphor-CCD systems. HAPS detectors show a relatively poor performance because of the additional scattering in the thick read-out chip. DSSD sensors have an ideal modulation transfer because of their counting architecture and capacity for on-line discrimination. Overall, both MAPS and DSSD sensors show an exceptional performance and these results highly recommend their application as imaging sensors in TEM.

5. Acknowledgements

This work was supported under EPSRC grant EP/C009509/1 and Framework 6 program for an Integrated Infrastructure Initiative, reference 026019 ESTEEM.

References

[1] Meyer R.R. and A Kirkland, Microscopy Research and Technique, 49, 269–280, 2000
[2] G Deptuch, A Besson, P Rehak, M Szelezniak, J Wall, M Winter and Y Zhu, Ultramicroscopy, 107, 674–684, 2007
[3] AR Faruqi, R Henderson and L Tlustos, Nuclear Instruments & Methods in Physics Research A, 546, 160-163, 2005
[4] G Moldovan, X Li, P Wilshaw and A Kirkland, IWORID 9 proceedings, in press, 2007